Publ. Astron. Obs. Belgrade No. 76 (2003), 117 - 131 *Invited lecture*

EARLY-TYPE GALAXIES: FROM SPECTRA TO DYNAMICAL ANALYSIS

SRDJAN SAMUROVIĆ[1,2,3]

[1] *Astronomical Observatory, Volgina 7, 11000 Belgrade, Serbia and Montenegro*

[2] *Dipartimento di Astronomia, via Tiepolo 11, 34131 Trieste, Italy*

[3] *Osservatorio Astronomico di Trieste, via Tiepolo 11, 34131 Trieste, Italy*
E–mail: srdjan@ts.astro.it

Abstract. A brief summary is given of some important aspects of observations and modelling of early-type galaxies. Photometric and long-slit spectroscopic observations, as well as two- and three-integral modelling of the early-type galaxy IC3370 are given as an example.

1. INTRODUCTION

Early-type galaxies (elliptical and lenticular galaxies) belong to the left-hand end of the Hubble's tuning-fork diagram. Shape of elliptical galaxies varies in form from round to elongated. One can use the simple formula $n = 10[1 - (b/a)]$, where (b/a) denotes the apparent axial ratio, to write the type of these galaxies: En. Therefore, E0 are round galaxies, and E6 are highly elongated systems. Research over last 20 years brought new knowledge about ellipticals and we now know that these galaxies are much more complex systems that they seemed. The elliptical galaxies contain little or no gas or dust. The old stars that are prevalent are cold, and therefore belong to the last spectral types. In the middle of the Hubble's diagram there is a class of galaxies designated as type S0, known as lenticular galaxies. They have a smooth central brightness condensation similar to an elliptical galaxy that is surrounded by a large region of less steeply declining brighteness. They have disks that do not show any conspicuous structure. Because of their appearance, and also because of their stellar content (e.g., spectral type), they look more like ellipticals rather than spiral galaxies. In this paper I will present observations and modelling of the galaxy IC3370 classified as E2-E3 (RC3, de Vaucouleurs et al., 1991).

2. OBSERVATIONS

IC3370 is a bright galaxy, classified as E2-E3 elliptical galaxy, absolute blue magnitude -21.4, heliocentric radial velocity 2930$\pm$24 km/s (see Fig. 1). It covers 2.9$\times$2.3 arcmin

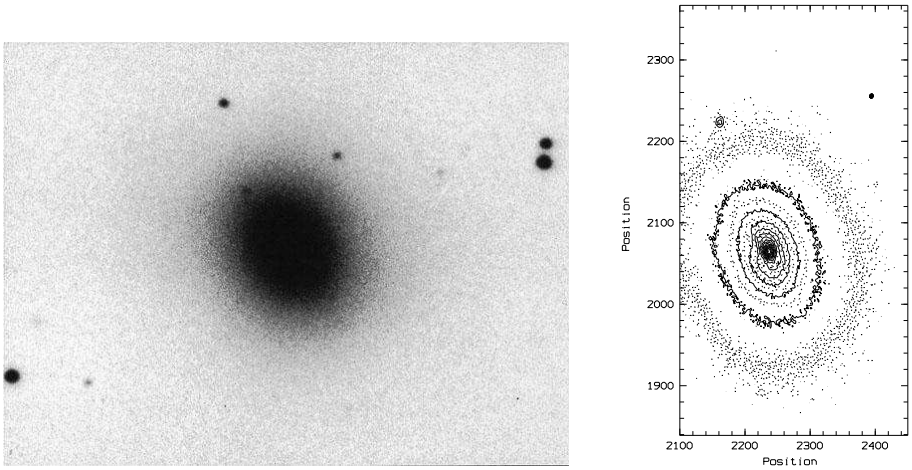

Fig. 1: Galaxy IC3370: image taken from NED (left) and contour plot (right)

on the sky (RC3). However, it is a rather unusual elliptical galaxy and according to Jarvis (1987, hereafter referred to as J87) it should be classified as S0pec (see below).

2. 1. PHOTOMETRIC OBSERVATIONS

I have used frames kindly provided by O. Hainaut using ESO NTT and EMMI in the RILD mode on July 3-4, 2002. The photometry of IC3370 is very interesting and it is given in detail in J87. I present here some additional elements that are complementary to that study and are of importance for the analysis that I am undertaking (more details will be available in Samurović and Danziger (2003)).

One should note that J87 took for the major axis the position angle (PA) of 40°, Carollo, Danziger and Buson (1993) took for the same axis PA of 51°, while the spectra in this study were taken using PA = 60°. The reason for these differences lies in a very particular photometry of this galaxy that has strong isophotal twisting as shown in J87 and in Fig. 2 (see position angle (P.A.) plot). This is the evidence of the fact that this galaxy is triaxial, because the isophotes of an axisymmetric system must always be aligned with one another (Binney and Merrifield, 1998, hereafter BM98). Fasano and Bonoli (1989) using sample of 43 isolated elliptical found that the twisting observed in these galaxies is intrinsic (triaxiality). Jarvis has taken the mean position angle of isophotes to be equal to $40 \pm 2°$ which is true for the data up to $80''$. However, at larger radii the PA tends to increase, so the usage of larger value of 60° (and 150° for the minor axis) is justified (see Fig. 2).

In Fig. 2 I present relevant photometrical data obtained using IRAF task `ellipse`: ellipticity, magnitude in B band for major axis (filled circles) and minor axis (open circles), a_4 parameter (fourth harmonic deviations from ellipse) and the position angles, as a function of distance. The value of a_4 is positive up to one effective radius[1] (for almost all values of radius), thus indicating that the isophotes are disky, while beyond one effective radius, isophotes become boxy since a_4 is negative. Since a_4 increases rapidly up to $\sim 5''$ this can lead to the conclusion of the embedded disk.

[1]Effective radius is the radius of the isophote containing half the total luminosity.

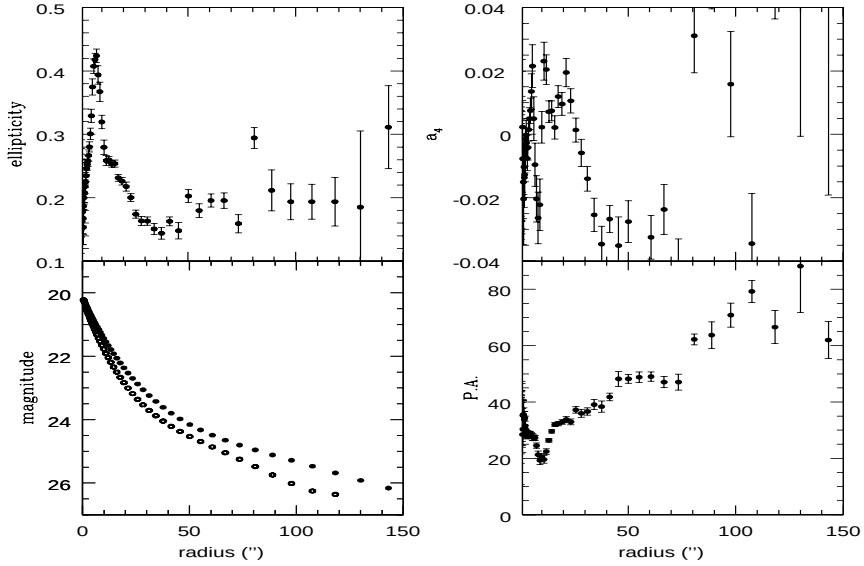

Fig. 2: Photometric profiles for IC3370. From top to bottom (left): ellipticity, surface brightness for the B filter (for major axis: full circles; for minor axis: open circles), (right): a_4 parameter and position angle.

The existence of the stellar disk was shown in J87. These photometric data will be necessary for the dynamical modelling that will be given below.

2. 2. LONG-SLIT SPECTRA

Long-slit spectra observations kindly provided by J. Danziger were taken during 1998 March 1-3, using ESO NTT and EMMI in the Red Medium Spectroscopy mode. The central wavelength was chosen to be near the Mg_2 feature: $\sim$ 5150 $\AA$. The range that was covered was $\sim$ 700 $\AA$. Several exposures were taken for different position angles: for the galactic major axis (P.A. = 60°) total exposure of 21,600 s, for the minor axis (P.A. = 150°) total exposure of 7,200 s. The spectra were rebinned at the telescope over 2 pixels giving a scale of 0.56 arcsec pixel $^{-1}$. I did standard data reduction procedures in ESO MIDAS: bias subtraction, division with the normalized dome flat field, filtering of the cosmic rays. Wavelength calibration was done using Helium-Argon comparison lamp spectra. Sky subtraction was done by taking average of 30 rows near the edges of the exposure frames. In the end the spectra were rebinned in the logarithmic scale. Also, spectra of several template stars were reduced as described above, continuum divided, and averaged over several rows in order to obtain one stellar template spectrum of high signal-to-noise ratio (S/N). In Fig. 3 I present a central galactic spectrum and a template star spectrum (K0 III star HR2701).

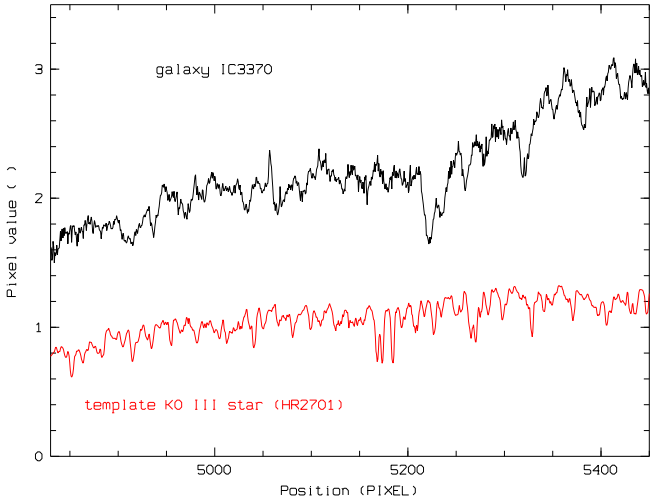

Fig. 3: Reduced central spectrum of the galaxy IC3370 (above) and template star (below). Spectra have been wavelength calibrated: x axis is in Angstroms. Note effects of velocity dispersion and redshift in the case of the galaxy; y axis is in arbitrary units.

3. STELLAR KINEMATICS: THEORETICAL APPROACH

In the case of IC3370, as in the case of all external galaxies, one cannot obtain data necessary for the reconstruction of the distribution function directly: one can observe line-of-sight velocities and angular coordinates. Since individual stars cannot be resolved, one has to deal with integrated stellar light that represents the average of the stellar properties of numerous unresolved stars that lie along each line of sight (LOS). Each star will have a slightly different LOS velocity, and therefore its spectral features will be shifted by a different amount: $\Delta u = c\Delta\lambda/\lambda = v_{\rm LOS}$. The final galaxy spectrum will be shifted and broadened, as shown in Fig. 3. First step in analysis of the shifts and broadenings is to define the line of sight velocity distribution (LOSVD, also called velocity profile, VP): this is a function $F(v_{\rm LOS})$ that defines the fraction of the stars that contribute to the spectrum that have LOS velocities between $v_{\rm LOS}$ and $v_{\rm LOS} + dv_{\rm LOS}$ and is given as $F(v_{\rm LOS})dv_{\rm LOS}$. Now, if one assumes that all stars have identical spectra $S(u)$ (where u is the spectral velocity in the galaxy's spectrum), then the intensity that is received from a star with LOS velocity $v_{\rm LOS}$ is $S(u - v_{\rm LOS})$. When one sums over all stars one gets:

$$G(u) \propto \int dv_{\rm LOS} F(v_{\rm LOS}) S(u - v_{\rm LOS}). \qquad (1)$$

This relation represents the starting point for a study of stellar kinematics in external galaxies (cf. BM98). The observer gets $G(u)$ for a LOS through a galaxy by obtaining its spectrum. If the galaxy is made of certain type of stars, one can estimate $S(u)$ using a spectrum of a star from the Milky Way galaxy (see Fig. 3,

lower part).

The solution of Eq. (1) seems rather simple. It would be enough to take its Fourier transform:

$$\tilde{F}(k) \propto \frac{\tilde{G}(k)}{\tilde{S}(k)} \tag{2}$$

where quantities with tilde sign are the Fourier transforms of the original functions. This is however very difficult task, since $\frac{\tilde{G}(k)}{\tilde{S}(k)}$ will be plagued by large errors that vary from point to point and the simple derivation of $F(v_{\rm LOS})$ will not be easy (for details, see BM98). Therefore, less direct methods have been invented to solve this problem.

First we can define the simplest properties of a LOSVD. Its mean value is given as:

$$\bar{v}_{\rm LOS} = \int dv_{\rm LOS} v_{\rm LOS} F(v_{\rm LOS}). \tag{3}$$

Its dispersion is given as:

$$\sigma^2_{\rm LOS} = \int dv_{\rm LOS} (v_{\rm LOS} - \bar{v}_{\rm LOS})^2 F(v_{\rm LOS}). \tag{4}$$

One possible solution is to assume that LOSVD has the Gaussian form. Sargent et al. (1977) invented the method known as Fourier Quotient Method, that has a problem of large errors for the ratio $\frac{\tilde{G}(k)}{\tilde{S}(k)}$ that vary from point to point. Cross-correlation method based on the calculation of the cross-correlation function between the galaxy and the stellar spectra was pioneered by Simkin (1974) and developed further by Tonry and Davis (1979).

LOSVD can be modeled as truncated Gauss-Hermite ($F_{\rm TGH}$) series that consists of Gaussian that is multiplied by a polinomial (van der Marel and Franx, 1993):

$$F_{\rm TGH}(v_{\rm LOS}) = \Gamma \frac{\alpha(w)}{\sigma} \exp(-\frac{1}{2}w^2) \left[1 + \sum_{k=3}^{n} h_k H_k(w)\right] \tag{5}$$

here Γ represents the line strength, $w \equiv (v_{\rm LOS} - \bar{v})/\sigma$, $\alpha \equiv \frac{1}{\sqrt{2\pi}} \exp(-w^2/2)$, where $\bar{v}$ and σ are free parameters. h_k are constant coefficients and $H_k(w)$ is a Gauss-Hermite function, that is a polynomial of order k. I will truncate the series at $k = 4$ (although higher values are also possible), for which the polynomials are:

$$H_3(w) = \frac{1}{\sqrt{6}}(2\sqrt{2}w^3 - 3\sqrt{2}w), \tag{6}$$

$$H_4(w) = \frac{1}{\sqrt{24}}(4w^4 - 12w^2 + 3). \tag{7}$$

Now LOSVD can be calculated by varying the values of $\bar{v}$, σ, h_3 and h_4 until the convolution of the function $F_{TGH}(v_{\rm LOS})$ with a template star spectrum best reproduces the observed galaxy spectrum. The optimal fit is then reached using a non-linear least-square fitting algorithm. If the form of the LOSVD is close to the Gaussian form, then $\bar{v}$ and σ will be approximately equal to $\overline{v_{\rm LOS}}$ and $\sigma_{\rm LOS}$. Parameters h_3 and h_4 are important because they measure asymmetric and symmetric departures from the

Gaussian. If one detects positive (negative) value of the h_3 parameter that would mean that the distribution is skewed towards higher (lower) velocities with respect to the systemic velocity. On the other hand, if one detects $h_4 > 0$ this means that the distribution is more peaked than the Gaussian at small velocities with more extended high-velocity tails; for $h_4 < 0$ the distribution is more flat-topped than the Gaussian. In the study of the dark matter in the early type galaxies the value of h_4 parameter plays a crucial role because it is constraining the level of tangential anisotropy which is extremely important since it is well known that the excess of tangential motions can mimic the existence of the dark matter haloes in these galaxies (Danziger 1997). The influence of changes in their values on the form of the LOSVD is given in Fig. 4.

4. STELLAR KINEMATICS: OBSERVATIONAL RESULTS

Internal part of the galaxy IC3370 can be considered 'disky' as it was shown before. Its rotation curve of the major axis is steeply rising to ~ 120 km s^{-1} within 20 arcsec and remains constant out to ~ 120 arcsec (> 3 effective radii). As it is usual in the case when a galaxy has a substantial rotational velocity, LOSVD is skewed, namely h_3 has the opposite sign to $\overline{v}_{\rm los}$. The values of h_4 parameter are consistent with zero value out to the ~ 3 R$_e$ thus indicating the lack of tangential anisotropies. Small deviations from the zero value are visible in the case of the minor axis. In Fig. 5 I present the extracted kinematical parameters of IC3370 for major (PA= 60°) and minor (PA= 150°) axes. Note that this galaxy shows signs of minor-axis stellar rotation: within $|r| \lesssim 10''$ velocity rapidly increases up to ~ 60 km s^{-1}. In Fig. 6 the reconstruction of LOSVD for IC3370 is given.

5. MODELLING

5. 1. TWO-INTEGRAL MODELLING

For the two-integral modelling procedures I used the modelling technique developed by Binney, Davies and Illingworth (1990, hereafter BDI), and subsequently used by van der Marel, Binney and Davies (1990), van der Marel (1990), and Cinzano and van der Marel (1994) (hereafter CvdM). Of all these papers only in CvdM the modelling includes also h_3 and h_4 parameters. Statler et al. (1999) used the modified version of this method to analyze mass distribution in NGC 1700. Here I briefly present the assumptions and the modelling steps.

Two-integral modelling is the first step in understanding of the dynamics of the elliptical galaxies, because in cases of small departures from triaxiality (which is far more probable, and true in case of IC3370 as it has been shown above), comparison of real systems with the models can provide useful insights. The assumptions of axisymmetry and the fact that the velocity dispersion tensor is everywhere isotropic are the starting points for the procedure that includes the following three steps (cf. BDI): (i) inversion of the luminosity profiles and obtaining three-dimensional luminosity density that provides the mass density (under assumption of constant mass-to-light ratio); (ii) evaluation of the potential and derivation of the velocity dispersion and azimuthal streaming (under assumptions that the form of the distribution function is $f(E, L_z)$, where E is the energy and L_z is the angular momentum of the individual star about the symmetry axis of the galaxy and that the velocity dispersion is isotropic) and (iii) comparison of the projected kinematical quantities from the model

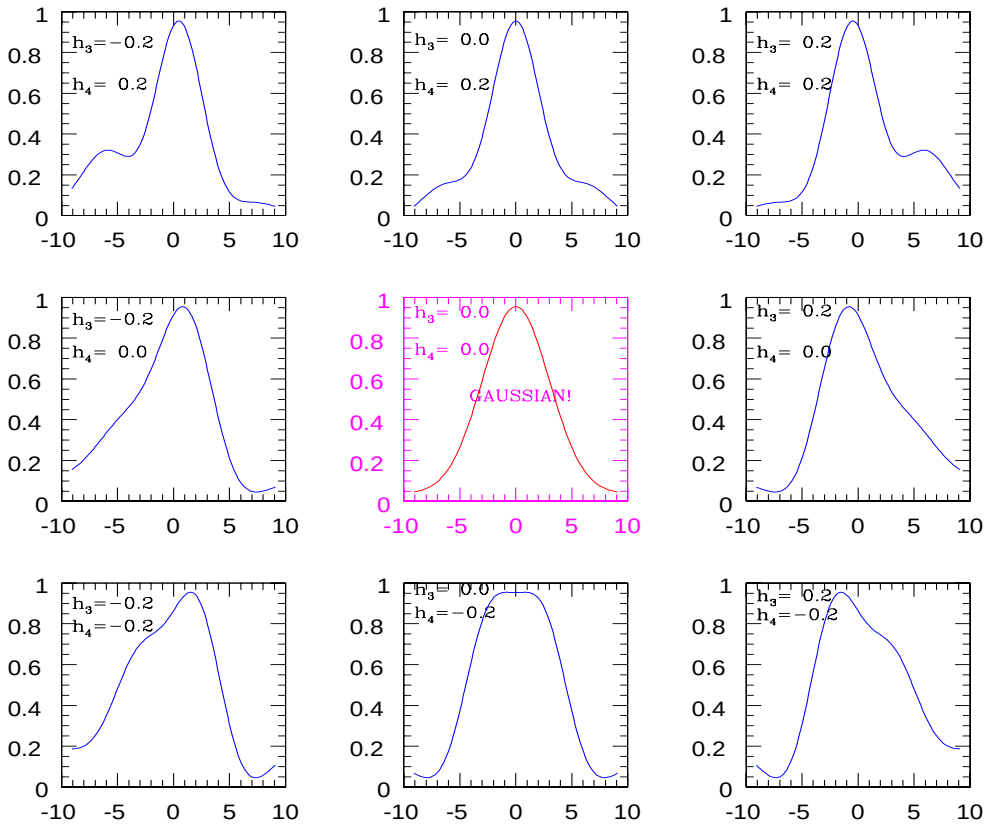

Fig. 4: Plots demonstrating various combinations of h_3 and h_4. Pure Gaussian is in the center (both h_3 and h_4 are equal to zero). h_3 parametrizes the skewness of the line profile, while h_4 measures whether the profile is more or less peaked than a Gaussian.

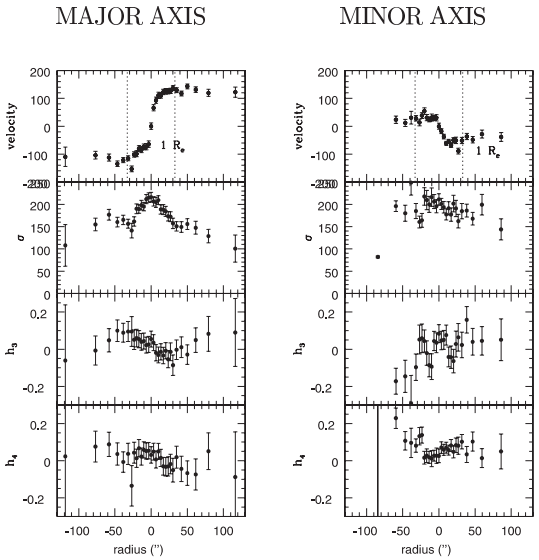

Fig. 5: Large scale kinematics for IC3370 for two different position angles. Left: major axis (PA = 60°) Right: minor axis (PA = 150°). From top to bottom: the mean line-of-sight velocity (in km/s), dispersion (in km/s), h_3 and h_4 parameters as a function of distance along different axes. The dotted lines indicate effective radius, $R_e \approx 31''$ in both cases.

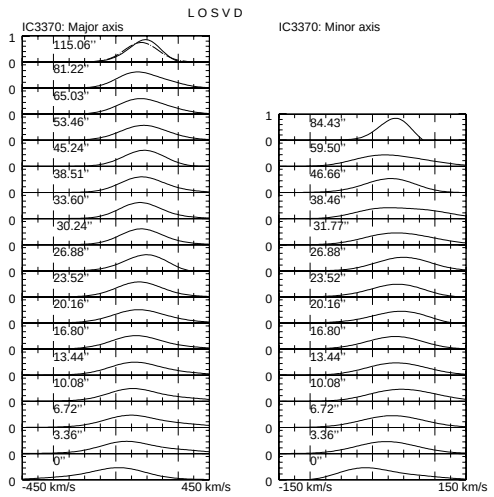

Fig. 6: LOSVD of IC3370 using data from Fig. 5. For a point at $115.06''$ the Gaussian is plotted as a dot-dashed line.

with the observed kinematic parameters; optionally, a disk, and/or a dark halo can be included in the modelling procedure.

The details of the modelling procedure are given in CvdM, and here I only briefly present some choices that I made and give the flowchart in Fig. 7. I assumed that the galaxy consists of a buldge and a disk; the dark matter halo is also included in the modelling procedure (see below). For the inclination I took $i = 50°$, because this value provided the best results in the modelling procedure. This value is in agreement with the value implied by the observed axial ratio of the isophotes, q_a: $i \geq \arccos q_a \gtrsim 46°$. I deprojected the photometry data using Lucy's algorithm to get the three-dimensional luminosity density. Then I obtained the mass density ρ using assumption of a constant mass-to-light ratio. The next step uses a three dimensional axisymmetric luminosity density, in order to evaluate the potential using a multipole expansion, and to solve the Jeans equations to find σ^2 and $\overline{v_\phi^2}$ for every point in the meridional plane. Since I assume that the distribution function is of the form $f(E, L_z)$ the second radial velocity moment, $\overline{v_R^2} \equiv \sigma_R^2$, and the second vertical velocity moment, $\overline{v_z^2} \equiv \sigma_z^2$ are everywhere equal and $\overline{v_R v_z} = 0$. The Jeans equations are:

$$\frac{\partial \rho \overline{v_z^2}}{\partial z} + \rho \frac{\partial \Phi}{\partial z} = 0 \tag{8}$$

$$\frac{\partial \rho \overline{v_R^2}}{\partial R} + \rho \frac{\partial \Phi}{\partial R} + \frac{\rho}{R}[\overline{v_R^2} - \overline{v_\phi^2}] = 0. \tag{9}$$

I solve them searching for unknowns $\overline{v_\phi^2}$ and $\sigma_R^2 = \sigma_z^2$. Using a free parameter, k, one can, as usual, assign a part of the second azimuthal velocity moment $\overline{v_\phi^2}$ to streaming:

$$\overline{v_\phi} = k\sqrt{\overline{v_\phi^2} - \sigma_R^2}.$$

Then I project the dynamical quantities on to the sky to get predictions.

My results of dynamical modelling are given in Fig. 8. It is obvious that this kind of modelling can provide rather good fit for the velocity in case one takes $k = 1$ (velocity dispersion is isotropic), adds disk potential and assumes that there is no dark matter. When one adds the potential of the dark matter (given as an isochrone Henon potential, as in Carollo and Danziger 1994) the fit for the major axis still remains good. The fit for $k = 0.6$ can be ruled out, while the fit for which disk potential is added and when there is no dark matter potential is good in the outer parts while in the inner parts it gives the velocity that is too large. The fits for dispersion, h_3 and h_4 are similar in four aforementioned cases. The dispersion along the major axis in the case in which one assumes the existence of the dark halo can be modeled using this approach, however a better fit is obtained without this assumption, since the dispersion continues to decrease. In the case of the minor axis, note that for the velocity all $k = 1$ models provide rather accurate values (again, $k = 0.6$ model can be ruled out). All four assumptions fail to produce observed dispersion values along the minor axis: observed values are always greater than the ones derived from the two-integral modelling. This two-integral model for given mass-to-light ratio underestimates minor axis dispersions. Model will be flattened by enhanced $\overline{v_\phi^2}$ which does not contribute to minor axis profile. Real galaxies are flattened by enhanced σ_R^2

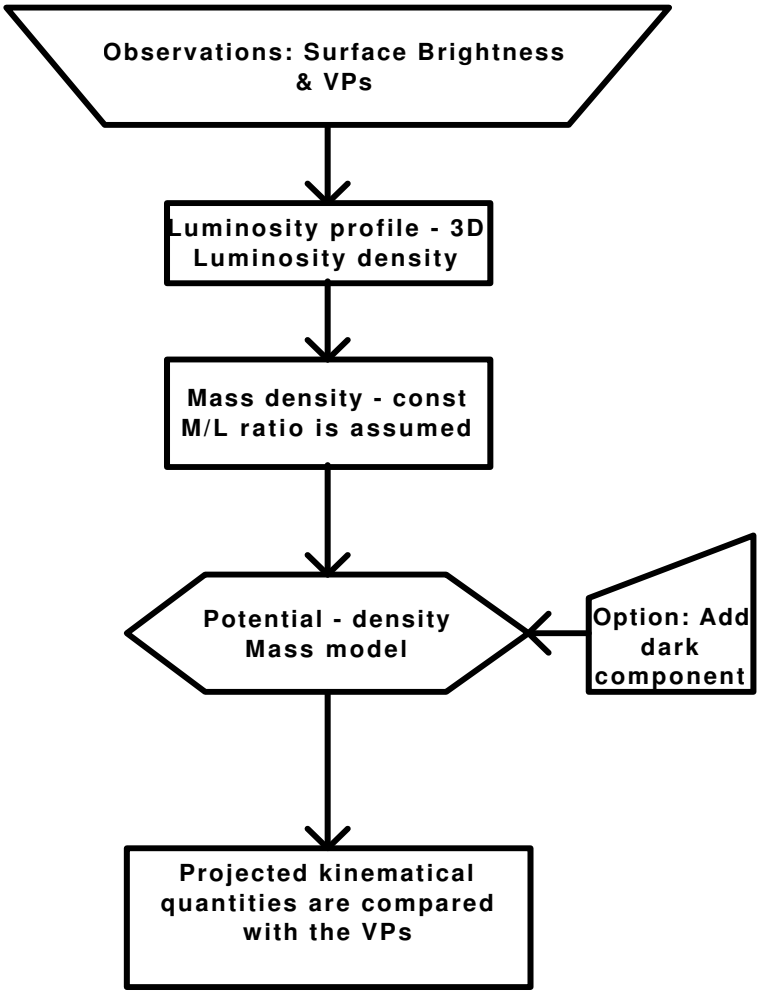

Fig. 7: Flowchart of two-integral modelling procedure. (VP stands for velocity profile).

which contributes on the minor axis. The radius of the disk that I have used to get a successful fit was 6 arcsec (0.9 kpc for $h = 0.71$).

The conclusion that can be drawn is that one can model IC3370 using two-integral modelling, but this approach is not completely satisfying because the observed dispersion on the minor axis deviates from the modeled one. Also, strictly speaking, this approach is not completely valid, since this galaxy is triaxial. The small values of h_4 parameter suggest that there are no big anisotropies in the outer part of the galaxy.

Judging from the results of this kind of modelling one cannot say firmly whether IC3370 is embedded in the dark halo, and one is faced with a situation similar to the one of NGC2663 from Carollo et al. (1995) paper. The inclusion of the dark matter in the modelling is not required, but as suggested in the analysis of S0 galaxy NGC 5866 for which the existence of the dark matter is not needed (Gerssen, 2000), the complete absence of dark halo is not likely. Another example found in the literature is the one of NGC 4472 (E2/S0 galaxy) for which the dispersion can be fitted both with and without the dark matter halo (Saglia et al., 1993).

5. 2. THREE-INTEGRAL MODELLING

For axisymmetric potentials one can have orbits that have three integrals of motion: E, L_z and I_3. There is no general expression for the third integral, I_3. The assumption that the distribution has the form $f = f(E, L_z, I_3)$ broadens the range of possible axisymmetric motions. Three-integral models are used for modelling triaxial systems. Schwarzschild (1979) invented a very powerful method that can be used for construction of axisymmetric and triaxial models of galaxies in equilibrium without explicit knowledge of the integrals of motion. The basic steps of this approach are the following: one specifies the mass model $\rho(r)$ and finds its potential and then constructs a grid of cells in a position space. Then initial conditions are chosen for a set of orbits and for every orbit one integrates the equations of motion for many orbital periods and measures how much time the orbit spends in each cell (that measures how much mass the orbit contributes to that cell). Finally, one needs to determine the non-negative weights for each orbit such that the summed mass in each cell is equal to the mass given by the original $\rho(r)$. For the last step one can use different methods; for example, Schwarzschild (1979) used linear programming. Non-negative least square (NNLS) method (Lawson and Hanson, 1974) was used in this work.

Schwarzschild original idea has recently been further developed: namely, models are now made that match the bulk kinematics and LOSVD of observed galaxies. Rix et al. (1997) used such approach to search for dark matter in elliptical galaxies. Cretton and van der Bosch (1999) used it to confirm the presence of nuclear black holes. Recently, Gebhardt et al. (2003) used orbit superposition method for detection of central black holes in 12 galaxies. These works deal with the axisymmetric modelling only. I have used Rix et al. (1997) algorithm to build a new Schwarzschild modelling code that uses the so-called self-organizing maps (SOMs) (Kohonen, 1997; Murtagh, 1995) to extract velocity profiles from the large orbits library. The flowchart is presented in Fig. 9.

The details of the modelling procedure are given in Rix et al. (1997). I give here only several important equations. Namely, one searches for non-negative superposition of orbital weights, γ_k, that best matches the observational constraints within the error bars:

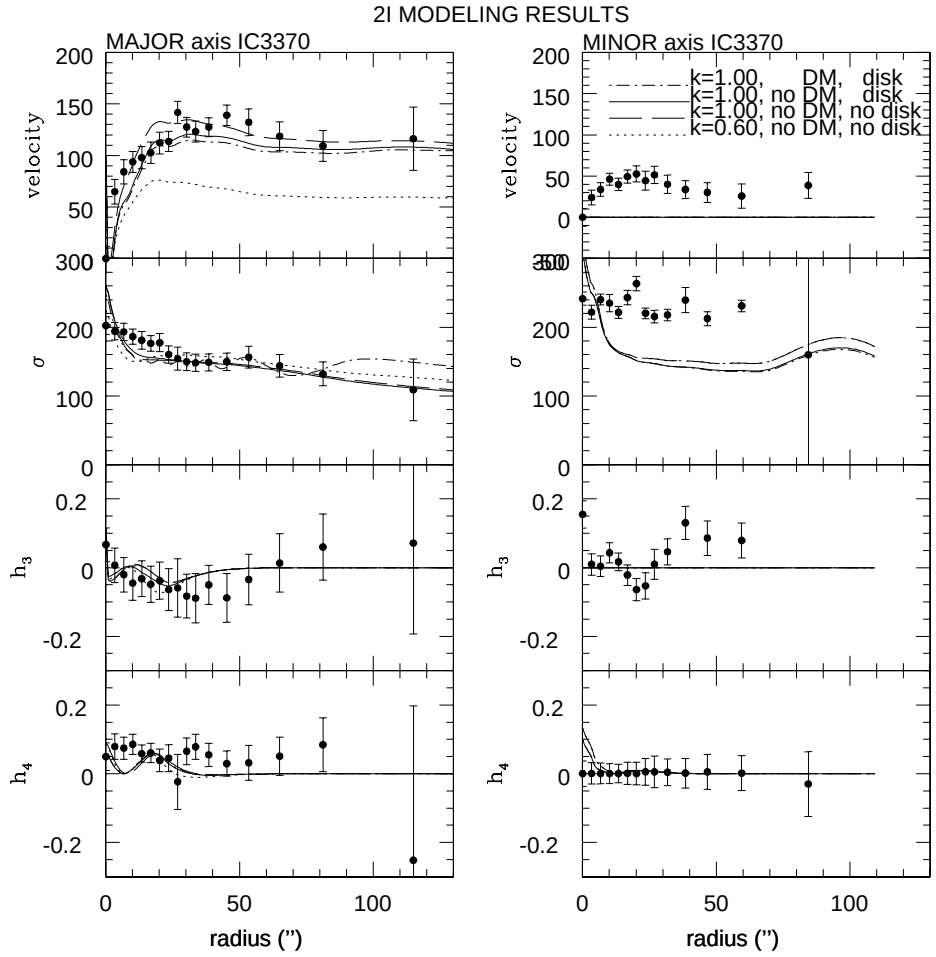

Fig. 8: Results of two-integral dynamical modelling of IC3370. Left: major axis modelling. Right: minor axis modelling. Solid lines represent cases with $k = 1$ with disk included and without dark matter. Dotted lines belong to $k = 0.6$ case, without the disk included and without the dark matter. Dot-dashed lines are for the case with $k = 1$ with the disk and dark matter included, and the dashed lines are for the case with $k = 1$ and no disk and no dark matter included (see text for details)

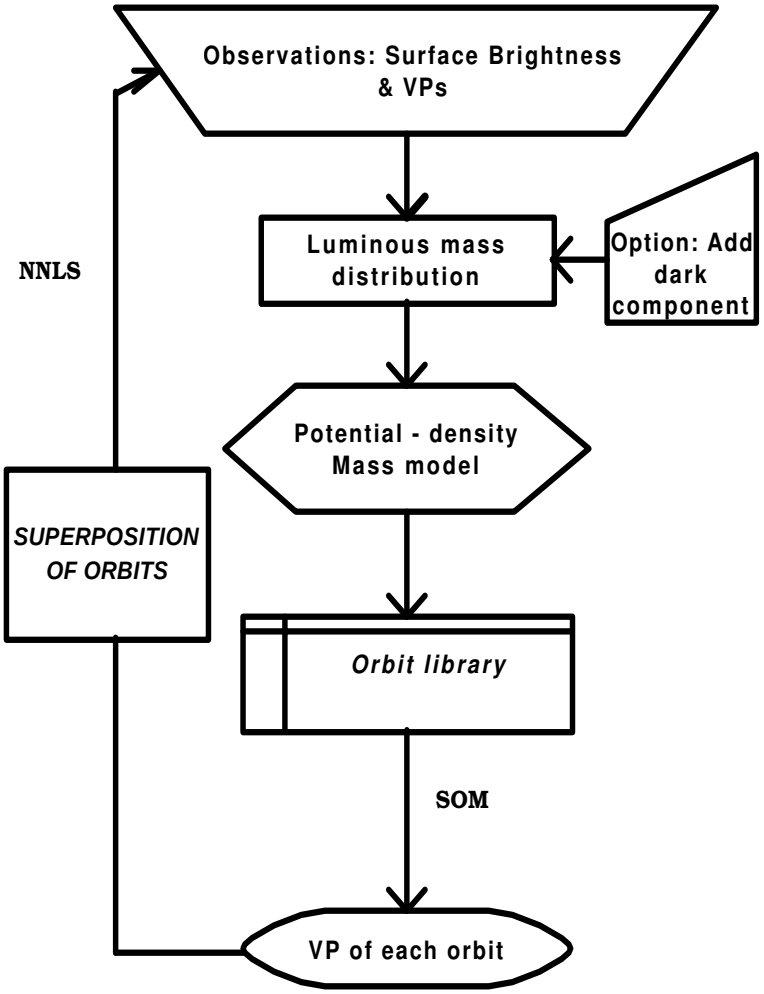

Fig. 9: Flowchart of three-integral modelling procedure. (SOM stands for self-organizing maps, NNLS for non-negative least squares).

$$\chi^2 \equiv \sum_{l=1}^{N_p}\left(\frac{M_l^{\rm obs}-\sum\gamma_k M_l^k}{\Delta M_l^{\rm obs}}\right)^2+\sum_{l=N_p+1}^{N_c}\sum_{m=1}^{4}\left(\frac{M_l^{\rm obs}h_{m,l}^{\rm obs}-\sum\gamma_k M_l^k h_{m,l}^k}{\Delta(M_l^{\rm obs}h_{m,l}^{\rm obs})}\right)^2, \quad (10)$$

Here, N_p are photometric constraints and $N_k = N_c - N_p$ are kinematic constraints (N_c is the number of constraint positions). Least squares problem that has to be solved for the occupation vector $(\gamma_1, \ldots, \gamma_{N_0})$, with the constraints $\gamma_k \geq 0$, for $k = 1, \ldots, N_0$ for $m = 1, 2, 3, 4$ is the following:

$$\begin{bmatrix} M_1^1 & \ldots & \ldots & M_1^{N_0} \\ M_2^1 & \ldots & \ldots & M_2^{N_0} \\ \vdots & \vdots & \vdots & \vdots \\ M_{N_p}^1 & \ldots & \ldots & M_{N_p}^{N_0} \\ M_{Np+1}^1 h_{1,N_p+1}^1 & \ldots & \ldots & M_{Np+1}^{N_0} h_{1,N_p+1}^{N_0} \\ \vdots & \vdots & \vdots & \vdots \\ M_{N_c}^1 h_{1,N_c}^1 & \ldots & \ldots & M_{N_c}^{N_0} h_{1,N_c}^{N_0} \\ \vdots & \vdots & \vdots & \vdots \\ \vdots & \vdots & \vdots & \vdots \\ M_{Np+1}^1 h_{M,N_p+1}^1 & \ldots & \ldots & M_{Np+1}^{N_0} h_{M,N_p+1}^{N_0} \\ \vdots & \vdots & \vdots & \vdots \\ M_{N_c}^1 h_{M,N_c}^1 & \ldots & \ldots & M_{N_c}^{N_0} h_{M,N_c}^{N_0} \end{bmatrix} \begin{bmatrix} \gamma_1 \\ \vdots \\ \vdots \\ \gamma_{N_o} \end{bmatrix} = \begin{bmatrix} M_1^{\rm obs} \\ M_2^{\rm obs} \\ \vdots \\ M_{N_p}^{\rm obs} \\ M_{Np+1}^{\rm obs} h_{1,N_p+1}^{\rm obs} \\ \vdots \\ M_{N_c}^{\rm obs} h_{1,N_c}^{\rm obs} \\ \vdots \\ \vdots \\ M_{Np+1}^{\rm obs} h_{M,N_p+1}^{\rm obs} \\ \vdots \\ M_{N_c}^{\rm obs} h_{M,N_c}^{\rm obs} \end{bmatrix} \quad (11)$$

Here, M denotes mass fractions, "obs" is related to the observed quantities. The total number of orbits is N_0.

I used this code for testing several astrophysically important potentials in a library of 729 orbits. Some very preliminary results are obtained for the logarithmic potential (Binney and Tremaine, 1987) that describes the flat rotation curves of galaxies. The model fits both velocity and velocity dispersion, because of the choice to fit them perfectly. For an axisymmetric potential that has the form

$$\Phi(R,z) = \frac{1}{2}v_0^2 \ln(R_c^2 + R^2 + z^2/q^2) \quad (12)$$

(R_c is the core radius, q describes the flattening of the potential and is taken to be $q = 0.7$ in this case) tube orbits cannot reproduce h_3 and h_4 parameters. For the triaxial potential:

$$\Phi(x,y,z) = \frac{1}{2}v_0^2 \ln(R_c^2 + x^2 + y^2/p^2 + z^2/q^2) \quad (13)$$

(here p and q are intrinsic axial ratios; they again describe flattening of the potential, and were taken to be $p = 0.8$ and $q = 0.7$ in this case) again h_4 cannot be fitted correctly. Fitting of h_3 with tube orbits can give some agreement, while fit for h_3 with box orbits is not satisfying. The conclusion is that widely used logarithmic potential

does not fit this galaxy, under aforementioned assumptions, although further checks are necessary (for example, using more orbits and using the regularization procedure). The results will be given in Samurović and Danziger (2003).

One possible way how the problem of triaxial modelling should be attacked would be to find the behavior of p and q parameters along the galaxy using observational constraints and to calculate potential for every point using these values (Eq. 13). This work is currently in progress.

Acknowledgements. I would like to thank my PhD thesis supervisors John Danziger and Francesca Matteucci for their encouragement and help. This work is a part of the project "Astrophysical Spectroscopy of Extragalactic Objects" supported by the Ministry of Science, Technologies and Development of Serbia. This research has made use of the NASA/IPAC Extragalactic Database (NED) which is operated by the Jet Propulsion Laboratory, California Institute of Technology, under contract with the National Aeronautics and Space Administration.

References

Binney, J.J., Davies, R.D., Illingworth, G.D.: 1990, *Astrophs. J.*, **361**, 78 (BDI).
Binney, J.J., Merrifield, M.R.: 1998 *Galactic Astronomy*, Princeton University Press (BM98).
Binney, J.J., Tremaine, S.D.: 1987, *Galactic Dynamics*, Princeton University Press.
Carollo, C.M., Danziger, I.J., Buson, L.: 1993, *Mon. Not. Roy. Astron. Soc.*, **265**, 553.
Carollo, C.M., Danziger, I.J.: 1994, *Mon. Not. Roy. Astron. Soc.*, **270**, 743.
Carollo, C.M., de Zeeuw, P.T., van der Marel, R.P., Danziger, I.J., Qian, E.E.: 1995, *Astrophys. J.*, **441**, L25.
Cinzano, P., van der Marel, R.P.: 1994, *Mon. Not. Roy. Astron. Soc.*, **270**, 325.
Cretton, N., van der Bosch: 1999, *Astrophys. J.*, **514**, 704.
Danziger, I.J.: 1997, *Dark and Visible Matter in Galaxies, ASP Conference Series, Vol. 117*, eds. Massimo Persic and Paolo Salucci.
De Vaucouleurs, G.: 1991, *Third Reference Catalogue of Bright Galaxies, version 3.9*
Fasano, G., Bonoli, C.: 1989, *Astron. Astrophys. Suppl. Ser.*, **79**, 291.
Gebhardt, K. et al.: 2003, *Astrophys. J.*, **583**, 92.
Gerssen, J.: 2000, *PhD Thesis*, University of Groningen.
Jarvis, B.: 1987, *Astron. J.*, **94**, 30 (J87).
Kohonen, T.: 1997, *Self-Organizing Maps*, Springer-Verlag.
Lawson, C.L., Hanson, R.J.: 1974, *Solving Least Squares Problems*, Englewood Cliffs, New Jersey: Prentice–Hall
Murtagh, F.: 1995, *Journal of Classifications*, **12**, 165.
Rix, H.-W., de Zeeuw, P.T., Cretton, N., van der Marel, R.P., Carollo, C.M.: 1997, *Astrophys. J.*, **488**, 702.
Saglia, R.P., Bertin, G., Bertola, F., Danziger, I.J., Dejonghe, H., Sadler, E.M., Stiavelli, M., de Zeeuw, P.T., Zeilinger, W.W.: 1993, *Astrophys. J.*, **403**, 567.
Samurović, S., Danziger, I.J.: 2003, in preparation.
Sargent, W.L.W., Schechter, P.L., Boksenberg, A., Shortridge, K.: 1977, *Astrophys. J.*, **212**, 326.
Schwarzschild, M.: 1979, *Astrophys. J.*, **232**, 236.
Simkin, S.M.: 1974, *Astron. Astrophys.*, **31**, 129.
Statler, T., Dejonghe, H., Smecker-Hane, T.: 1999, *Astron. Journal*, **117**, 126.
Tonry, J., Davis, M.: 1979, *Astron. Journal*, **84**, 1511.
van der Marel, R.P.: 1991, *Mon. Not. Roy. Astron. Soc.*, **253**, 710.
van der Marel, R.P., Binney, J.J., Davies, R.D.: 1990, *Mon. Not. Roy. Astron. Soc.*, **245**, 582.
van der Marel, R.P., Franx, M.: 1993, *Astrophys. J.*, **407**, 525.